

# Response of Soil Phage Communities and Prokaryote–Phage Interactions to Long-Term Drought

Cong Liu, Zhijie Chen, Xinlei Wang, Yijun Deng, Linfang Tao, Xuhui Zhou, and Jie Deng\*



Cite This: *Environ. Sci. Technol.* 2025, 59, 3054–3066



Read Online

ACCESS |

Metrics & More

Article Recommendations

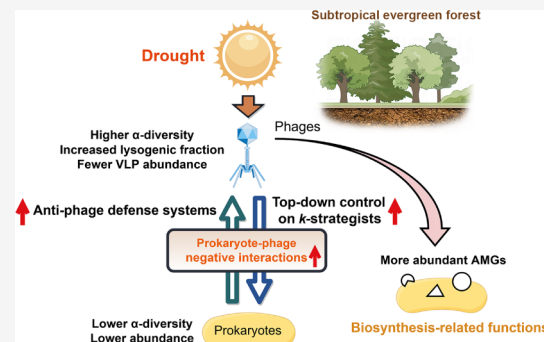
Supporting Information

**ABSTRACT:** Soil moisture is a fundamental factor affecting terrestrial ecosystem functions. In this study, microscopic enumeration and joint metaviromic and metagenomic sequencing were employed together to investigate the impact of prolonged drought on soil phage communities and their interactions with prokaryotes in a subtropical evergreen forest. Our findings revealed a marked reduction in the abundances of prokaryotic and viral-like particles, by 73.1% and 75.2%, respectively, and significantly altered the structure of prokaryotic and phage communities under drought. Meanwhile, drought substantially increased the fraction of prokaryotic communities containing lysogenic phages by 163%, as well as the proportion of temperate phages. Nonetheless, drought likely amplified negative prokaryote–phage interactions given the nearly doubled proportion of negative links in the prokaryote–phage co-occurrence network, as well as the higher frequency and diversity of antiphage defense systems found in prokaryotic genomes. Under drought, soil phages exerted greater top-down control on typical soil *k*-strategists including *Acidobacteria* and *Chloroflexi*. Moreover, phage-encoded auxiliary metabolic genes may impact host metabolism in biosynthesis-related functions. Collectively, the findings of this study underscore the profound impact of drought on soil phages and prokaryote–phage interactions. These results also emphasize the importance of managing soil moisture levels during soil amendment and microbiome manipulation to account for the influence of soil phages.

**KEYWORDS:** drought, soil phages, host–phage interaction, global climate change, soil moisture

## 1. INTRODUCTION

Viruses are the most diverse and abundant biological entities on Earth and are present in soils at densities ranging from  $10^7$  to  $10^{10}$  per gram according to microscopic enumeration.<sup>1,2</sup> Bacteriophages are the primary components of total soil viruses.<sup>2</sup> There has been increasing recognition that soil phages play crucial roles in regulating microbial community dynamics and the hosts' metabolic functions.<sup>3–5</sup> Phages can directly lyse host cells, releasing intracellular organic matter and influencing nutrient uptake and turnover in living microorganisms.<sup>6,7</sup> Additionally, phage-encoded auxiliary metabolic genes (AMGs) may alter host metabolism, affecting host adaptation and biogeochemical cycling of various elements.<sup>8–11</sup> The preservation and reproduction of phages in soils are regulated by a range of environmental factors, including those associated with global climate change.<sup>12</sup> Specifically, climate change in recent decades has increased the frequency and intensity of regional drought, leading to reduced soil moisture levels.<sup>13</sup> This alteration in soil moisture not only affects the structure and function of soil microbial communities<sup>14,15</sup> but is also expected to substantially impact soil phages and their interactions with host microbes.<sup>12</sup> In soils with distinct moisture levels, the extent of phage top-down regulation on host microbes can differ greatly, which further impacts



processes including soil organic matter mineralization<sup>16,17</sup> and carbon sequestration.<sup>18</sup> Hence, elucidating the response of soil phages and host–phage interactions to drought is essential for understanding and predicting soil biogeochemical processes under current and future climate changes.

Past studies suggested that drought may influence the structure, abundance, and lifestyle of soil phage communities. A recent global soil metagenomic analysis underscored the key role of soil moisture in shaping phage community diversity.<sup>19</sup> Microscopic enumeration revealed a positive correlation between soil moisture and the abundance of virus-like particles (VLPs) in soil,<sup>20</sup> possibly due to increased bacterial abundance and enhanced diffusion in moist soils, which together improve the chances of host exposure to phages and promote the production of more virulent phages. Drought may also affect the lysis and lysogeny lifestyle of bacteriophages. Generally, lysogeny is expected to enhance the survival of both phages

Received: August 21, 2024

Revised: January 19, 2025

Accepted: January 22, 2025

Published: February 7, 2025



ACS Publications

© 2025 American Chemical Society

and hosts<sup>21,22</sup> and may improve host fitness under adverse environmental conditions.<sup>23–25</sup> For instance, the soil viruses from Antarctica's dry valleys were predominantly temperate phages.<sup>26</sup> However, a study comparing soil phages across grasslands with different historical precipitation regimes revealed that lower precipitation favored a higher abundance and diversity of temperate phages.<sup>27</sup> Therefore, the patterns and mechanisms by which soil phages and host–phage interactions respond to drought remain unclear.

In complex microbial and phage communities, the investigation of host–phage interactions is crucial for understanding the effect of phages on prokaryotic community structure and functions, which can be facilitated by several approaches.<sup>28,29</sup> Hosts may be predicted through searches against microbial genome databases and matching phage sequences with CRISPR (clustered regularly interspaced short palindromic repeats) spacer sequences in host genomes.<sup>30,31</sup> The presence and abundance of adaptive immune systems in host microbes can reflect phage predation pressure.<sup>32–34</sup> Additionally, coexistence networks<sup>35–37</sup> of host microbes and phages can provide insights into potential host–phage interactions. For example, a bacteria–T4-like phage network constructed from serial surface ocean samples revealed complex relationships among these entities.<sup>28</sup> Similarly, in an investigation of the coral-associated microbiome during a white plague disease outbreak, host–phage coexistence network analysis revealed an important role of phages in controlling stress-associated symbiotic bacteria.<sup>38</sup> In soils, although previous studies have revealed the possible effect of soil moisture on phage lifestyle and diversity,<sup>27,39</sup> it remains unclear how soil prokaryote–phage interactions respond to changes in soil moisture.

Host–phage interactions can also be mediated through phage-encoded AMGs, which may compensate for hosts' metabolic burden by aiding adaptation under stressed conditions.<sup>40</sup> For example, in peatland soils, phage AMGs involved in carbohydrate synthesis and degradation may influence soil carbon cycling.<sup>41,42</sup> In paddy soils, AMGs associated with phosphorus and nitrogen cycling, e.g., organic phosphorus uptake and degradation, nitrogen transport and metabolism, etc., have been identified.<sup>43</sup> In soils contaminated with organochlorine pesticides, the presence of AMGs linked to pesticide degradation may contribute to increased bacterial growth at subinhibitory pesticide concentrations.<sup>44</sup> Similarly, in chromium-contaminated soils, phages may facilitate the transfer of AMGs associated with heavy metal resistance among bacterial hosts.<sup>45</sup> Further exploration of soil phage AMGs is essential for advancing our understanding of phage-mediated cellular and biogeochemical processes.

Despite the significant rise in soil virology studies in recent years, most rely on identifying viral sequences within soil metagenomic data sets. However, viral sequences typically constitute only a small fraction (0 to 3%) of these data sets. In contrast, metaviromic sequencing, which involves the enrichment of soil viruses prior to sequencing, has demonstrated clear advantages, offering higher coverage and better representation of soil viromes.<sup>46,47</sup> In this study, both metaviromic and metagenomic approaches were employed to investigate the response of soil phage communities within soil aggregates to long-term drought. Our research was conducted in a long-term experimental field located in the Tiantong National Forest in Eastern China, where rainfall-reduction treatment has been ongoing since 2012. To elucidate the

impact of drought on soil phages, soil VLP abundances and lifestyle strategies were assessed using microscopic enumeration. Then, the differences in phage community structure, prokaryote–phage ecological network, prokaryote antiphage defense systems, and phage-encoded AMGs were compared between drought and control treatments. We hypothesize that drought could (1) substantially reduce the abundances of VLPs and the  $\alpha$ -diversity of phage communities and (2) increase the fraction of temperate phages and the associated AMGs, hence promoting positive prokaryote–phage interactions. Overall, this study aims to uncover the patterns by which soil phages and prokaryote–phage interactions respond to long-term drought and to enhance understanding of phage regulatory mechanisms over prokaryotic communities in the context of global climate change.

## 2. MATERIALS AND METHODS

**2.1. Sampling Site Description and Sample Collection.** Soil samples were gathered in the long-term rainfall reduction experimental field located in Tiantong National Forest Ecosystem Observation and Research Station (29°52' N, 121°39' E, 163 m above sea level) in Zhejiang Province, Eastern China, in June 2018. The region is characterized by a subtropical monsoon climate, with a hot summer and a cold winter. Mean annual temperature and precipitation are 16.2 °C and 1374.7 mm, respectively. The soil type is Acrisol, with its texture being a clay loam with 6.8% sand, 55.5% silt, and 37.7% clay.<sup>48</sup> The experimental field was established in 2012, with details of the field setup described by Zhou et al.<sup>48</sup> Briefly, for the drought treatment, concave transparent polycarbonate boards were evenly fixed at a height of 1.5–3.5 m above ground in the drought plots and covered roughly 70% of the total area. The control plots were maintained under natural conditions without any disturbance. Three plots were set up for each treatment and were randomly allocated. The size of each plot was 25 × 25 m, and the intervals among plots were at least 5 m. A buffer region of 2.5 m width was set around each plot. A 2 m-deep trench was dug around each plot, and polycarbonate isolation panels were placed around the plot to prevent lateral runoff of rainfall. The soil samples were collected in June 2018. After removing litter and surface debris, the top 10 cm of soil was sampled from each plot using soil corers (5 cm in diameter) with an inner bulldozer device to ensure the integrity of the soil core.<sup>49,50</sup> Aggregate fractionations were separated into four size fractions: > 2 mm (S1, large macroaggregate), 1–2 mm (S2, medium macroaggregate), 0.25–1 mm (S3, small macroaggregate), and <0.25 mm (S4, microaggregate) using the “optimal moisture” sieving approach.<sup>51</sup> The samples from triplicate plots were combined for the viral nucleic acid extraction. The four samples for drought (DR) and four samples for control (CK) were subjected to metagenomic and metaviromic sequencing, respectively.

**2.2. Epifluorescence Microscopy Counting and Prophage Induction Assays.** Extraction of soil prokaryotic cells and VLPs was conducted according to the procedures previously described.<sup>16</sup> Briefly, the SM solution (100 mM NaCl, 10 mM MgSO<sub>4</sub>, 50 mM Tris, and 0.01% Gelatin, pH 7.5) was used as the extraction buffer. After mixing with the soil, the soil sludge was vortexed at high speed for 20 min and centrifuged at 2500g for 8 min. Supernatant was transferred to 50 mL centrifuge tubes and passed through 5  $\mu$ m filter membranes to remove small particles.

For the prophage induction assay, the obtained suspension was treated with 1  $\mu$ g/mL (final concentration) mitomycin C (regarded as the induction group) and without mitomycin C (regarded as the control).<sup>52</sup> All samples were wrapped with aluminum foil to protect them from light exposure and incubated at room temperature for 18 h before enumeration of prokaryotic cells and VLPs. Burst size (BZ) was calculated with the equation:  $BZ = \frac{V_i - V_0}{B_0 - B_i}$ . The lysogenic fraction (LF) among the host community was calculated as  $LF (\%) = \frac{V_i - V_0}{B_2 \times B_0} \times 100$ .  $B_i$  and  $V_i$  represented prokaryotic and viral abundances in the induced sample, respectively;  $B_0$  and  $V_0$  represented prokaryotic and viral abundance in the control sample, respectively.

Enumeration of prokaryotic cells and VLPs was conducted using methods previously described<sup>16,20</sup> in **Text S1**.

**2.3. Soil Physicochemical Analysis and Enzymatic Assays.** Soil physicochemical properties and enzymatic activities were determined using the same methods previously described.<sup>50</sup> In brief, the activities of four hydrolases: cellobiohydrolase (CBH),  $\beta$ -1,4-glucosidase ( $\beta$ G), acid phosphatase (AP), and  $\beta$ -1,4-N-acetylglucosaminidase (NAG), as well as two oxidases: polyphenol oxidase (PPO) were measured according to the methods by Saiya-Cork et al.<sup>53</sup> Total carbon (TC) and total nitrogen (TN) of the soil samples were measured by using an elemental analyzer (Elemental Analyzer, Vario EL III, Germany). The nonhydrolyzed carbon (NHC) content was assessed according to the procedures in Su et al.<sup>50</sup> The soil moisture content is shown in **Figure S1**.

**2.4. Metagenomic and Metaviromic DNA Extraction and Sequencing.** **2.4.1. Metagenome.** Soil total DNA was extracted from a 0.5 g soil sample using the DNeasy PowerSoil Pro Kit (Qiagen, Germany) according to the manufacturer's instructions. Metagenomic sequencing was performed on the Illumina NovaSeq 6000 platform (150 bp, paired-end mode) at Guangdong Magigene Biotechnology Co., Ltd. Metagenomic sequencing yielded 71,005,801–80,770,019 reads per sample (average 76,555,847 reads/sample).

**2.4.2. Metavirome.** Briefly, 3 g of soil sample was suspended in 10 mL of SM solution (100 mM NaCl, 10 mM MgSO<sub>4</sub>, 50 mM Tris, and 0.01% Gelatin, pH 7.5), together with 2 g of glass beads (2 mm diameter), and vortexed at 2800 rpm for 15 min, followed by centrifugation at 4000g for 5 min. The above processes were repeated three times, and the supernatant was collected and combined. The supernatant was subsequently filtered through 0.22  $\mu$ m filter membranes to remove host cells and concentrated using Amicon centrifugal ultrafiltration tubes (30k, Millipore, Germany). The viral particles were precipitated by PEG8000 at 4 °C, and the viral concentrate was treated with DNase I (Thermo Fisher, USA) to eliminate free DNA. The universal primers for the 16S rRNA gene (515F/806R) were used to confirm the absence of prokaryotic DNA residue. Viral DNA was extracted with the QIAamp DNA Micro Kit (Qiagen, Germany), and amplified with the REPLI-g Single Cell kit (Qiagen, Germany). The quality of amplified products was assessed by 1% agarose gel, Qubit 4.0 (Thermo Fisher Scientific, USA), and Nanodrop One (Thermo Fisher Scientific, USA). Metaviromic sequencing was performed on the Illumina Novaseq 6000 platform (150 bp, paired-end mode) at the Guangdong Magigene Biotechnology Co., Ltd. The metagenomic and metaviromic sequence data were deposited at the NODE database (<https://www.biosino.org/node>) under project OEP005425. Metaviromic sequencing

yielded 33,462,460–35,311,237 reads per sample (average 33,940,596 reads/sample).

**2.5. Metagenome Assembly, Taxonomic Assignment, and Functional Annotation.** Trimmomatic (v0.39) was used for raw data processing.<sup>54</sup> The contigs were assembled using Megahit (v1.2.9) with default parameters as --min-contig-len 500 for prokaryotes.<sup>55</sup> Then, Prodigal (v2.6.3)<sup>56</sup> was used to predict open reading frames (ORFs) using the meta option.<sup>56</sup> CD-HIT (v4.8.1)<sup>57</sup> was adopted to remove redundancy and obtain the unigenes (i.e., the nucleotide sequences coded by unique and continuous genes) catalog with parameters: -c 0.95 -aS 0.9. Afterward, the gene catalogs were mapped with clean data using BBMap (v38.18, <https://github.com/BioInfoTools/BBMap>) with default parameters to determine the abundances of genes in each sample. ORFs were annotated with reference to NCBI RefSeq databases using Diamond (v2.0.5.143)<sup>58</sup> (e-value  $\leq 1 \times 10^{-5}$ ). The gene functions were annotated according to the KEGG database<sup>59</sup> (e-value  $\leq 1 \times 10^{-5}$ ).

**2.6. Metavirome Assembly, Phage Identification, Clustering, Taxonomical, and Functional Annotation.** Trimmomatic (v0.39) was used for raw data processing<sup>54</sup> and BWA (v0.7.17) was used to remove possible host genome sequences.<sup>60</sup> The contigs were assembled using Megahit (v1.2.9) with default parameters as --min-contig-len 500 for phages.<sup>55</sup> The contigs longer than 3 kb were retained. Then, CD-HIT (v4.8.1)<sup>57</sup> was adopted to remove redundancy and obtain the unigenes (i.e., the nucleotide sequences coded by unique and continuous genes) catalog with parameters: -c 0.95 -aS 0.85. Phage sequences were identified from the assembled contigs through a combination of three mainstream tools: (1) VirSorter2 (v2.2.4) with "max\_score  $\geq 0.9$ ";<sup>61</sup> (2) DeepVir-Finder (v1.0) with  $p \leq 0.05$  and score  $\geq 0.9$ ;<sup>62</sup> (3) VIBRANT (v1.2.1).<sup>63</sup> CheckV (v1.0.1) was applied to assess the quality of phage genomes with at least one viral hallmark gene and completeness  $\geq 15$ .<sup>64</sup> Next, the identified phage contigs were estimated by BWA (v0.7.17) to compare clean reads, and the reads per kilobase of exon model per million mapped reads (RPKM) of each contig were calculated to obtain the phage abundance. Prodigal (v2.6.3) was used for the prediction of phage genes using the meta option,<sup>56</sup> and the genes were annotated according to GhostKOALA<sup>65</sup> by GHOSTX search against a nonredundant set of KEGG GENES (the virus database). Taxonomic assignment of phage contigs was performed using PhaGCN based on the latest ICTV classification tables.<sup>66</sup> Afterward, DRAM-v (v1.4.0) was used for phage-encoded AMG identification with default parameters.<sup>67</sup> The genes with auxiliary scores of 1–3 and AMG flag of -M and/or -F were considered as AMGs.<sup>67</sup> The BPROM server (<http://www.softberry.com/>) was used to predict the promoter of AMGs.<sup>68</sup> Phyre2 (v2.0) was used for secondary and tertiary structural homology searches for each AMG.<sup>69</sup>

**2.7. Prokaryote–Phage Ecological Interaction Analysis.** **2.7.1. Prediction of Phage Hosts.** Three approaches (CRISPR-match, tRNA match, and genome homology match) were adopted to improve the accuracy and comprehensiveness of phage host prediction.<sup>70</sup> (1) The prokaryotic contigs were used for searching CRISPR spacers by the CRISPR recognition tool (CRT, v2.0).<sup>71</sup> The identified CRISPR spacers were compared with phage contigs using BLASTn (v2.6.0+), and those passing the thresholds of  $\geq 95\%$  identity and  $\leq 2$  single nucleotide polymorphisms (SNPs) were selected to predict putative phage hosts. (2) tRNA genes in phage contigs were

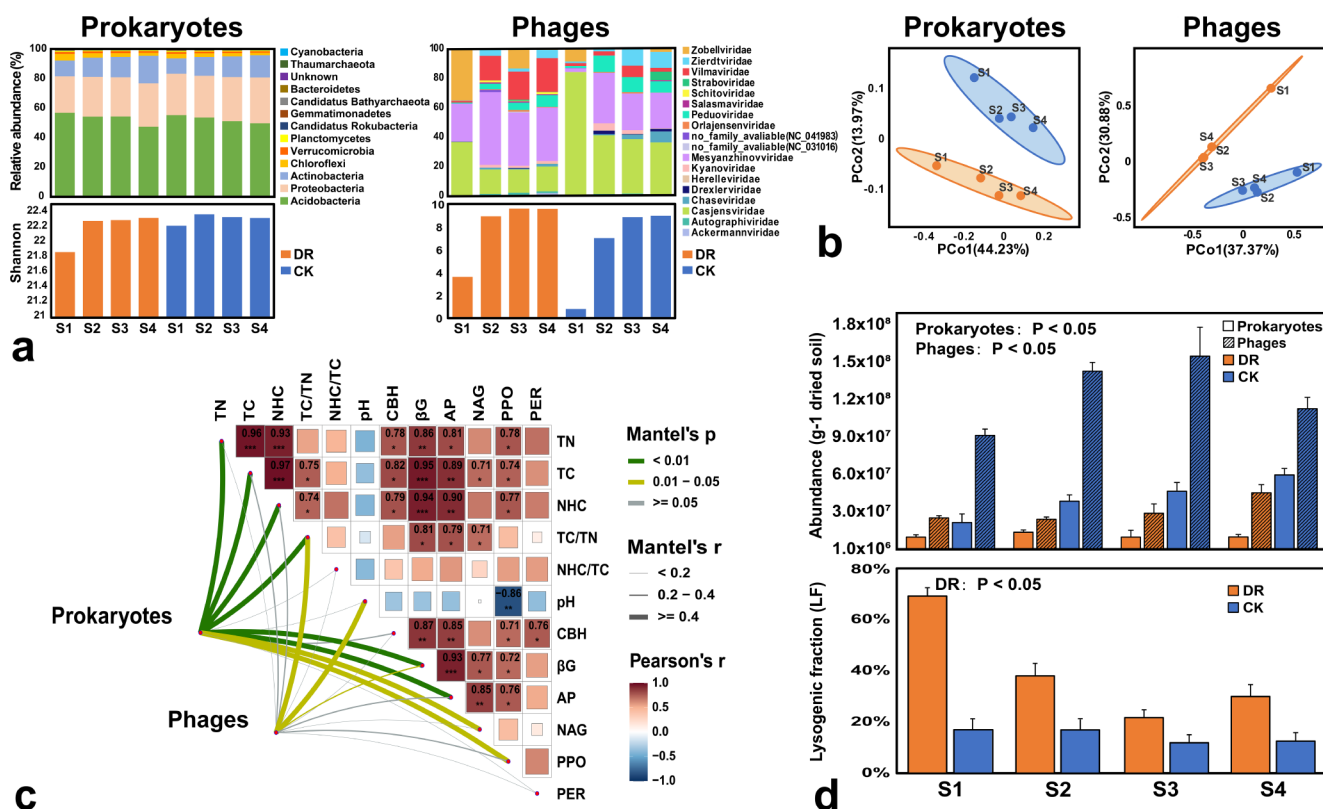


**Figure 1.** Changes of prokaryotic and phage community composition in soil aggregates (S1: large macroaggregates,  $> 2$  mm; S2: medium macroaggregates, 1–2 mm; S3: small macroaggregates, 0.25–1 mm; and S4: microaggregates,  $< 0.25$  mm). “DR” and “CK” represent “drought” and “control” treatment, respectively. (a) Composition of prokaryotic and phage communities. (b) PCoA of prokaryotic and phage community structures. (c) Mantel correlation between prokaryotic and phage communities with soil physicochemical properties and enzyme activities. “TC”, “TN”, and “NHC” represent “total carbon”, “total nitrogen”, and “non-hydrolyzed carbon” content in the samples, respectively. (d) The prokaryotic and VLP abundances, as well as LF of the prokaryotic communities.

predicted by tRNAscan-SE (v2.0.7) with default settings and blasted against the prokaryotic sequences using BLASTn, keeping only the best hits with at least 95% sequence identity.<sup>72</sup> (3) Phage genomic signatures in microbial genomes, lysogens, were identified via a search against the prokaryotic contigs through BLASTn with the following parameters: bitscore  $\geq 50$ , e-value  $\leq 10^{-3}$ , identity  $\geq 70\%$ , and matching length  $\geq 2500$  bp.<sup>73</sup>

**2.7.2. Phage Lifestyle Prediction.** The temperate and virulent lifestyles of phages were first determined by identifying lysogenic signals (transposase, integrase, excisionase, resolvase, and recombinase proteins) based on protein sequences from Pfam (v35.0)<sup>74</sup> using “hmmscan” from HMMER (v3.1b2) with an E value  $\leq 0.00001$ . The phages without lysogenic signals were further screened with PhaTYP (Score  $\geq 0.75$ )<sup>75</sup> and VIBRANT (v1.2.1)<sup>63</sup> to distinguish temperate and virulent lifestyles. Since many phage genomes did not have high completeness, it is possible that the proportion of temperate phages may be underestimated.

**2.7.3. Analysis of Defense Systems and Prokaryote–Phage Network.** Defense-finder (V1.2.0) was used to identify antiphage defense systems in hosts.<sup>76</sup> The interaction ecological network between soil prokaryotes and phages was constructed by the “ggClusterNet” package.<sup>77</sup> The parameters were set as follows: “Pearson” correlation,  $r = 0.8$ ,  $p = 0.05$ , layout\_net = “model\_Gephi.2”. The network was visualized by Gephi, version 0.10.1.

**2.8. Statistical Analyses.** Data were statistically analyzed using the R platform (v4.0.3). The  $\alpha$  and  $\beta$  diversity analyses of prokaryotes and phages were conducted using “vegan”<sup>78</sup> and “ggplot2”<sup>79</sup> packages in R. The Mantel test was used to calculate the pairwise correlations among the Bray–Curtis dissimilarities of prokaryotic and phage communities, and the Euclidean distances of environmental factors. The correlation between prokaryotic and phage OTU numbers was analyzed using the “ggbpubr” package.<sup>80</sup> The phage lineages with significantly different abundance distributions under drought were identified using the “edgeR” package (FDR  $< 0.05$ ).<sup>81</sup> The schematic diagram of sample collection and data processing is presented in Figure S2.

### 3. RESULTS

**3.1. Changes in Prokaryotic and Phage Communities in Soil Aggregates under Drought.** Long-term drought showed significant effects on both soil prokaryotic and phage community compositions (Figure 1a, b). A total of 8,297,594 mOTUs were obtained from the metagenomic profiles, and the dominant prokaryotic phyla included *Acidobacteria*, *Proteobacteria*, *Actinobacteria*, etc. Drought treatment significantly decreased the relative abundances of *Gammaproteobacteria*, *Betaproteobacteria*, and *Deltaproteobacteria*, while increasing the abundance of *Actinobacteria* (Figure S3). From the metaviromic profiles, a total of 6688 vOTUs longer than 3 kb were identified. Only 3.4% of all vOTUs were taxonomically annotated based on the latest ICTV classification rules, among

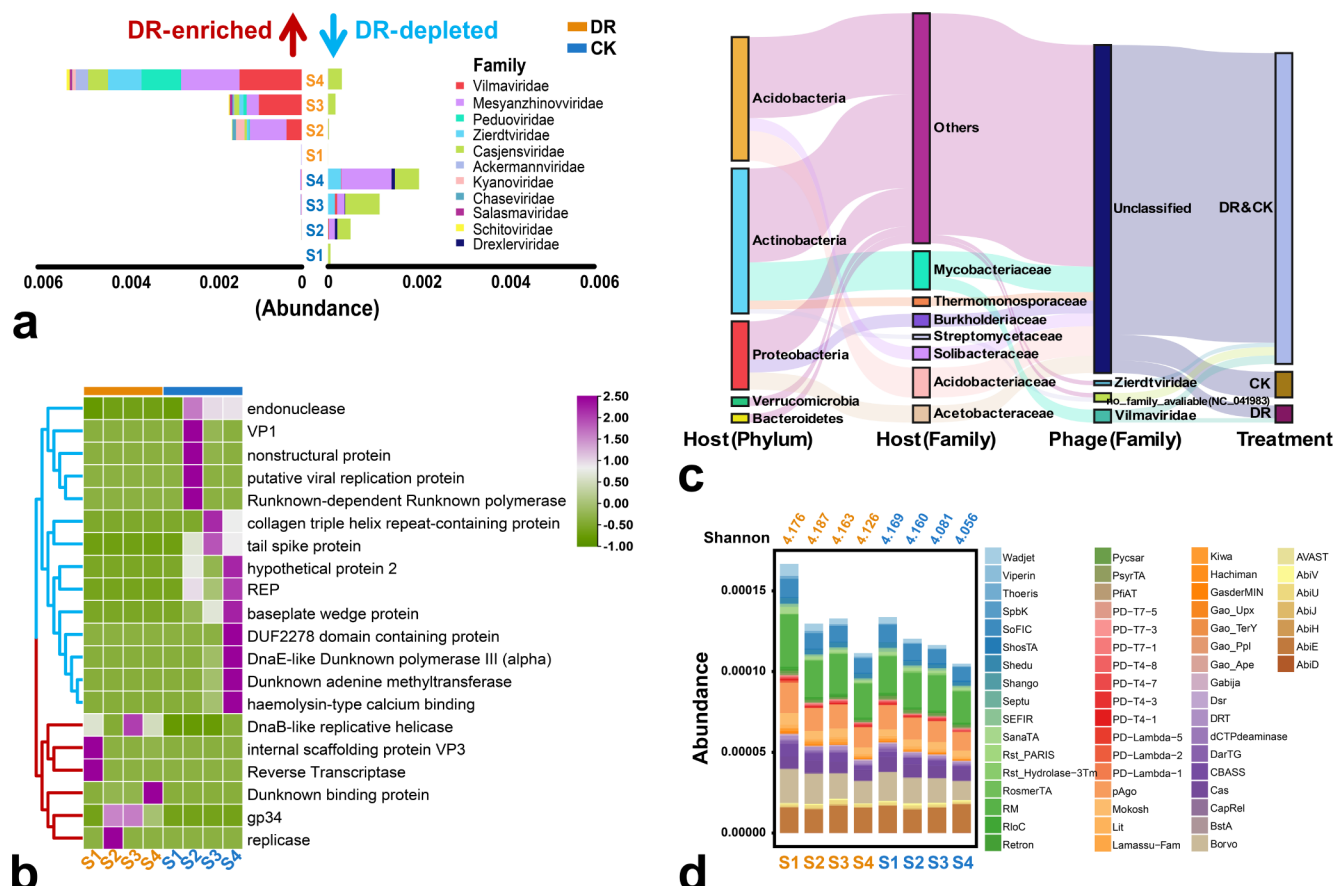


**Figure 2.** Analysis of soil prokaryote–phage interactions. (a) The phage taxa showing significant abundance changes under drought. (b) Functions of phage genes showing significant abundance changes under drought. (c) Predicted host–phage associations. (d) The composition of antiphage defense systems carried by soil prokaryotes.

which the major phage families included *Mesyanzhinoviridae*, *Casjensviridae*, *Vilmaviridae*, *Peduoviridae*, etc (Figure 1a). The proportions of classifiable vOTUs in the samples are shown in Figure S4.

Multivariate analyses suggested that the phage communities were more susceptible to drought (Table S1). Drought resulted in 1.6% decrease in  $\alpha$ -diversity for prokaryotic communities but 24.1% increase for phage communities (Figure 1a). The numbers of mOTUs and vOTUs were significantly correlated ( $r = 0.79, p < 0.05$ ) (Figure S5). Based on epifluorescence microscopic counting, drought lowered prokaryotic and free VLP (virus-like particle) abundances by 73.1% and 75.2%, respectively, while increasing the lysogenic fraction of prokaryotic communities by 163.0% (Figure 1d). Mantel analysis demonstrated that prokaryotic community structure was significantly related to TC, TN, NHC, TC/TN,  $\beta$ G, AP, NAG, and PPO; phage community structure was strongly associated with pH and TC/TN (Figure 1c). The above observations suggested different responses of soil phages to drought compared to prokaryotes.

The phage taxa and phage functional genes differentially responded to drought (Figure 2a,b). Among all vOTUs, 9.4% were significantly enriched under drought, including those associated with the families of *Vilmaviridae*, *Peduoviridae*, and *Zierdtviridae*, whereas 10.3% of the vOTUs were enriched under control, including those associated with *Casjensviridae* (Figures S6 and 2a). In terms of phage functional genes, those involved in DNA replication were enriched under drought,

whereas those related to endonucleases, structural and nonstructural proteins, adenine methyltransferases, etc., were enriched under control (Figure 2b).

**3.2. Soil Host–Phage Associations and Host-Encoded Antiphage Defense Systems.** The putative host–phage linkages (Figure 2c) and the antiphage defense systems carried by prokaryotes (Figure 2d) were investigated across all samples. Specifically, the phage contigs associated with *Zierdtviridae*, *Vilmaviridae*, and *no\_family\_available* (NC\_041983) were linked to five host phyla and seven host families based on matches of the CRISPR spacer sequences, tRNA sequences, as well as reference genome sequences (Figure 2c). The host phyla covered *Acidobacteria*, *Actinobacteria*, *Proteobacteria*, *Verrucomicrobia*, and *Bacteroidetes*, all of which were among the dominant soil prokaryotic phyla (Figure 1a). A total of 83 host–phage pairs were matched.

Based on the metagenomic profiles, a total of 58 types (82 subtypes) of antiphage defense systems were characterized, among which Restriction-modification systems (RM), Borvo, AbiE, pAgo, SoFIC, Cas, Mokosh, CBASS, Wadjet, and Shedu were of the top 10 highest abundances. A significant proportion (53%) of these defense systems were associated with unknown hosts, while the rest were distributed across the major phyla of prokaryotic communities, including *Acidobacteria*, *Proteobacteria*, *Actinobacteria*, and so on (Figure S7). Both the overall abundance and  $\alpha$ -diversity of the defense systems were higher under drought compared with the control (Figure 2d). Specifically, the antiphage defense systems

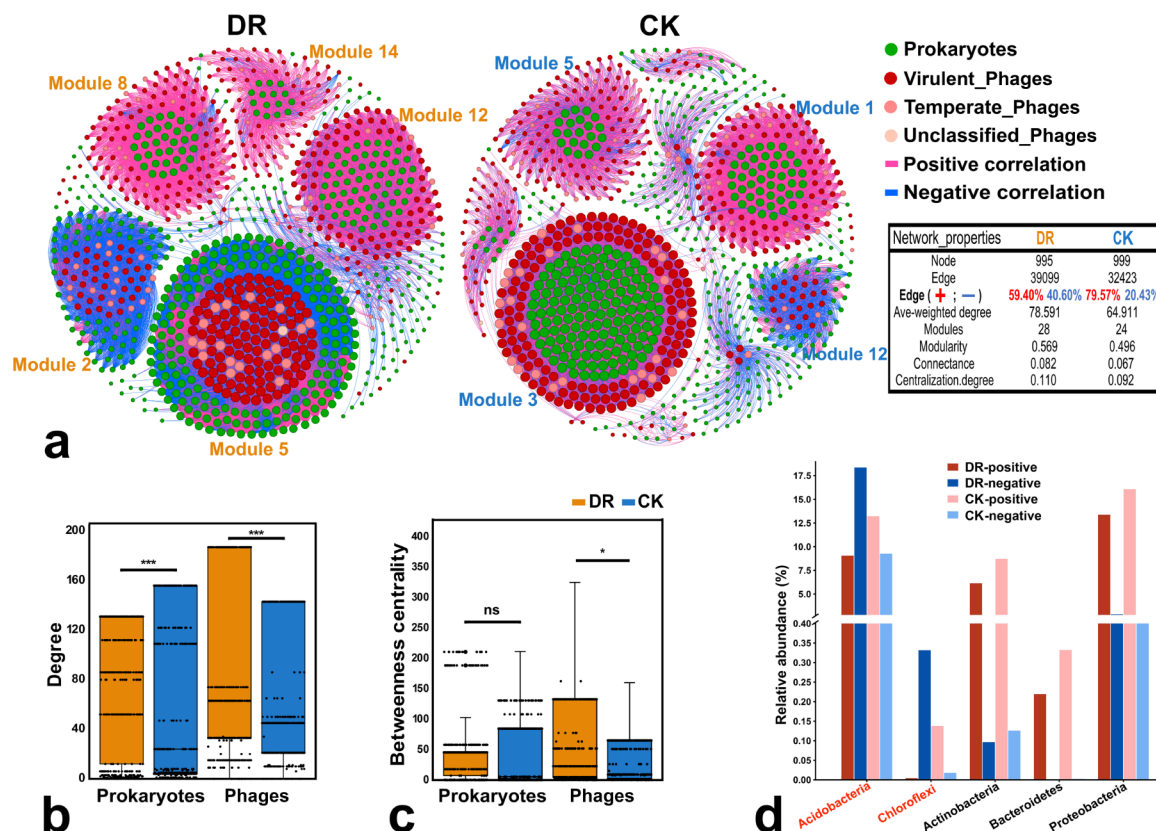


**Figure 3.** Ecological network among prokaryotes and phages. (a) The prokaryote–phage co-occurrence network under drought and control. (b) The degree and (c) betweenness centrality of prokaryotic and phage nodes in the network. (d) The proportion of positive and negative prokaryote–phage links associated with the dominant bacterial groups under drought and control.

associated with RM, Borvo, pAgO, Mokosh, CBASS, Wadjet, and Shedu showed increased abundances under drought (Figure 2d), which may suggest a change in phage predation stress.

**3.3. Ecological Network Among Soil Prokaryotes and Phages.** The ecological network analysis was performed to further assess the interactions among soil prokaryotes and phages (Figure 3). Notably, the proportion of negative correlations between prokaryote and phage nodes was markedly higher under drought compared with control (Figure 3a), likely suggesting more counteracting interactions between prokaryotes and phages. The betweenness centrality and degree of nodes exhibited a significant positive correlation (Figure S8). Among the major modules, those characterized by prokaryotic nodes with higher degree and centrality were dominated by positive correlations, whereas those characterized by phage nodes with higher degree and centrality were dominated by negative correlations (Figure 3a). Under drought, the prokaryotic nodes had significantly lower degree and betweenness centrality, whereas the phage nodes had significantly higher degree and betweenness centrality (Figure 3b and 3c). The above results suggested increased significance of the phage nodes in the network structure under drought. In addition, for the two bacterial groups (*Acidobacteria* and *Chloroflexi*), the proportion of negative prokaryote–phage links showed a marked increase under drought (Figure 3d).

**3.4. Phage-Encoded AMGs under Long-Term Drought.** A total of 899 phage-encoded AMGs were identified, mainly involving carbon utilization (249), organic nitrogen (44), MISC (hybrid types, 26), and unassigned (523)

functional categories. Drought increased the diversity of overall AMGs, especially the number of AMGs carried by temperate phages (Figure 4b). The AMGs involved in pathways including chromosome and associated proteins, DNA replication proteins, cysteine and methionine metabolism, folate biosynthesis, and purine metabolism, etc., were enriched under drought; whereas those involved in amino sugar and nucleotide sugar metabolism, O-antigen nucleotide sugar biosynthesis, fructose and mannose metabolism, polyketide sugar unit biosynthesis, ascorbate and aldarate metabolism, streptomycin biosynthesis, etc., were enriched under control (Figure 4a). Among the predicted AMG genes, *DNMT1*, *GCH1*, *queD*, and *purD* were enriched under drought; *rfbB*, *GME*, *TALDO1*, and *UGDH* were enriched under the control (Figure 4c). Figure 5 illustrates various pathways involving phage AMGs. Under drought conditions, these include tetrahydrobiopterin biosynthesis, adenine ribonucleotide biosynthesis, and pyrimidine deoxyribonucleotide biosynthesis. Under control, pathways including dTDP-L-rhamnose biosynthesis and the pentose phosphate pathway were featured.

## 4. DISCUSSION

Soil moisture is a key factor regulating soil nutrient availability, microbial metabolism, and the associated biogeochemical processes. In this study, through epifluorescence counting and joint metaviromic and metagenomic sequencing approaches, the profound impact of drought on soil phages and host–phage interactions was further revealed. Hence, soil moisture not only directly regulates soil microbial community structure and functions but also indirectly through its effect on

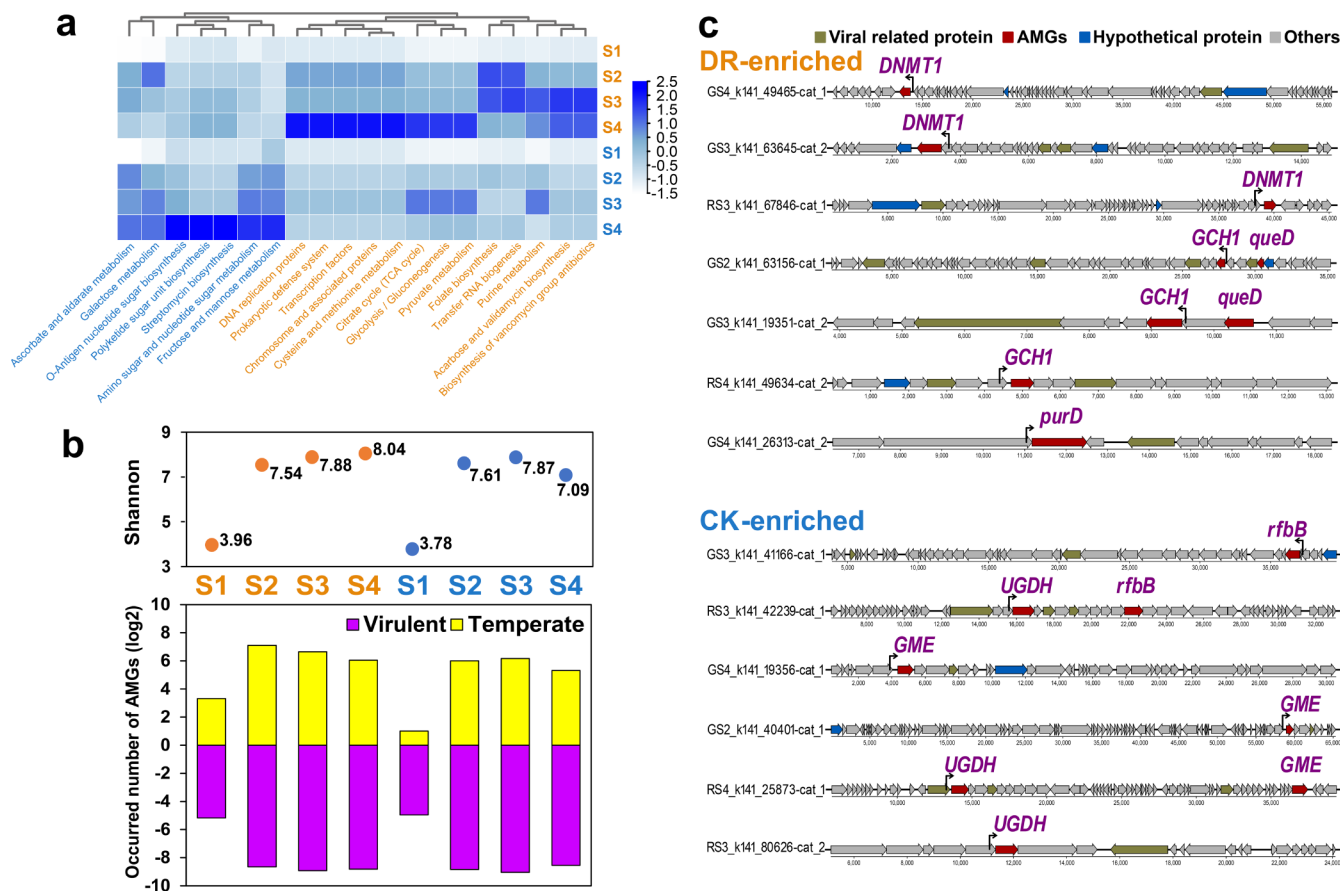


**Figure 4.** Phage-encoded AMGs under drought and control. (a) Heatmap of the AMGs classification in KEGG pathways. (b) Number and diversity of the AMGs carried in temperate and virulent phage contigs. (c) Genome and protein structures of selected AMGs under drought and control.

soil phages. Improved understanding of the associated processes and mechanisms may facilitate better prediction of ecosystem function response to drought under the climate change scenario.

**4.1. The Change of Lifestyle and  $\alpha$ -Diversity of Soil Phages under Drought.** Former studies have revealed that lysogeny is favored when bacterial hosts exhibit slow growth rates.<sup>82–87</sup> In this study, an increased lysogeny was observed under long-term drought treatment (Figure S9), which was consistent with the decreased growth rate of microorganisms, evidenced by reduced soil respiration,<sup>88,89</sup> decreased enzyme activities,<sup>43,44</sup> as well as a decreased number of prokaryotic cells as determined by microscopic enumeration (Figure 1d). Additionally, the increase in temperate phages may be linked to drought-associated stress conditions such as osmotic stress and ion toxicity.<sup>90</sup> Although related research remains limited, a study reported an increased lysogenic fraction of bacterial communities under elevated chromium (Cr) stress in Cr-contaminated soils.<sup>45</sup> Nonetheless, the ecological and molecular mechanisms regulating phage life cycles in soils await further investigation.

Interestingly, the change in  $\alpha$ -diversity of soil phage communities was opposite to that of prokaryotic communities, which was contrary to our initial hypothesis. Specifically, a 1.6% decrease in Shannon diversity of prokaryotic communities was observed, yet the Shannon diversity of soil phages increased by 24.1% (Figure 1a). Both temperate and virulent phages exhibited increased Shannon diversity under drought

(Figure S10). This pattern may be linked to the significant decline of *r*-strategists, e.g., *Proteobacteria* in particular, under drought at this site<sup>50</sup> (Figures 1a and S3). Members of this taxon are usually fast-growing organisms that thrive on unstable soil nutrients and maximize growth rates when resources are plentiful.<sup>91–93</sup> Their decreased abundance under drought may lead to a corresponding decline in phages targeting these fast-growing hosts, which are often associated with large burst sizes. Consequently, the reduced dominance of these specific phages allowed a greater diversity of phages to be detected with the same sequencing effort, resulting in greater evenness and the observed increase in phage diversity (Figure S11).

**4.2. Drought Promoted Negative Interactions between Soil Prokaryotes and Phages.** A few past studies have demonstrated that drought could greatly impact the structure of soil microbial networks.<sup>14,94</sup> However, the effect of drought on prokaryote–phage networks has remained under-explored. Chow et al. constructed the bacteria–T4-like phage network for the surface ocean, revealing 74% of positive correlations between bacteria and T4-like phages,<sup>28</sup> despite the common recognition of T4-like phages as virulent phages. In this study, it is worth noting that among the major modules, those dominated by positive links were characterized by prokaryotes with higher degree and centrality, whereas those dominated by negative links were characterized by phages with higher degree and centrality. These likely correspond to different prokaryote–phage interacting mechanisms, where the

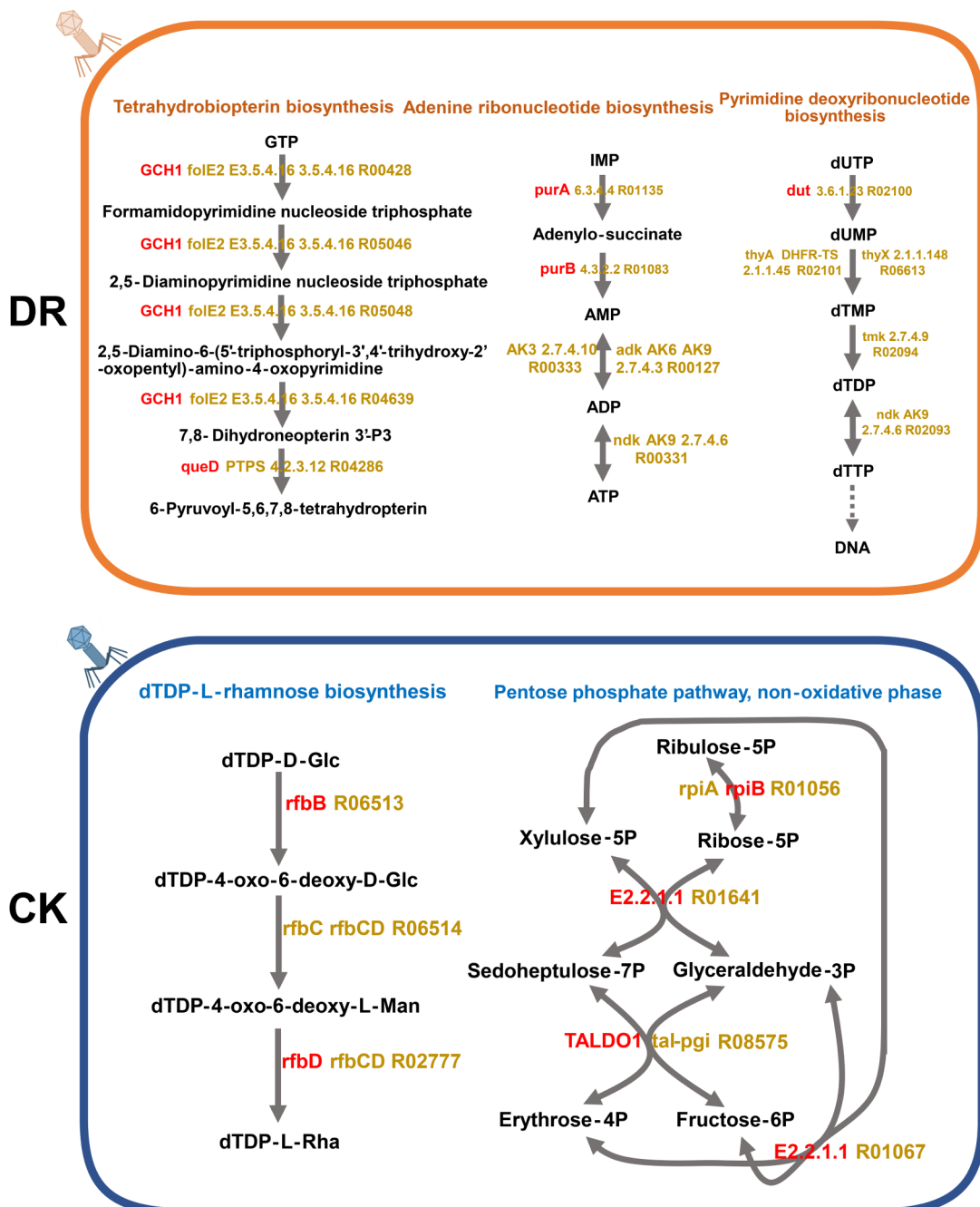


**Figure 5.** Functional illustration of AMGs enriched under drought and control. The genes in red are encoded by phages.

former may suggest the change in phage abundances follows that of host abundances, and the latter may suggest phages cut down host abundances through top-down regulation. Under long-term drought, the proportion of negative links almost doubled (40.60% under drought compared to 20.43% under control) in the prokaryote–phage network, and the degree and centrality of phage nodes also significantly increased (Figure 3), likely reflecting elevated “virulence” of the phage communities on the prokaryotic hosts. This phenomenon is interesting and seems contrary to common expectation as well as our hypothesis that wet soils would enhance cell lysis by phages.<sup>12</sup> Here, the increase in negative prokaryote–phage links under drought was primarily associated with *k*-strategists *Acidobacteria*<sup>95,96</sup> and *Chloroflexi*<sup>97</sup> distributed in major

modules of the drought network (Figures 3d and S12). Meanwhile, for these two bacterial groups, the proportion of positive prokaryote–phage links showed a marked decrease under drought (Figure 3d). Hence, the prokaryote–phage links for typical *k*-strategists *Acidobacteria* and *Chloroflexi* changed from being dominated by positive links under control to being dominated by negative links under drought, which may suggest a shift in prokaryote–phage interaction mechanisms, and that soil phages exerted elevated top-down control especially on *k*-strategists under drought.

Consistent with the overall increased negative links in the prokaryote–phage network under drought, both the abundance and diversity of antiphage defense systems carried by prokaryotes also increased (Figure 2d). A former study by Wu

et al.<sup>27</sup> reported that soil from regions with lower precipitation contained lower frequencies of antiphage defense systems. However, only CRISPR-Cas-associated systems were profiled. In this study, drought enriched genes associated with the widely distributed restriction-modification systems (RM)<sup>98</sup> that attack foreign DNA entering the cell,<sup>99</sup> the single-gene antiphage system Borvo,<sup>100</sup> the prokaryotic Argonaute homologue (pAgo)<sup>101</sup> that uses guide RNAs and/or ssDNAs for targeted inhibition,<sup>102</sup> as well as the cyclic oligonucleotide-based antiphage signaling system (CBASS) that promotes cell death upon phage infection,<sup>103</sup> etc. Since prokaryotic immune systems constantly undergo active evolution, their distribution is generally considered closely associated with phage activities.<sup>32</sup> In addition, many of the defense systems and genes are also subject to horizontal gene transfer, which facilitates fast adaptation under phage predation stress.<sup>104</sup> Here, the higher frequency and diversity of defense systems under drought were in line with the higher phage diversity as well as the overall increased proportion of negative links in the prokaryote–phage network.

In a relevant study, microbial necromass C was assessed in this experimental field and showed a significantly higher contribution to total soil organic C (SOC) under drought.<sup>105</sup> Furthermore, the fraction of bacterial necromass C in total microbial necromass C significantly elevated under drought<sup>105</sup> and exhibited an increasing trend with drought duration.<sup>106</sup> These results are consistent with our finding of enhanced host–phage “antagonism”, and suggest bacterial mortality due to phage activities may affect microbial necromass accumulation and SOC dynamics.

#### 4.3. Both Virulent and Temperate Phages Carried AMGs.

Both temperate and virulent phages are known to carry AMGs, which could affect host metabolism and potentially influence biogeochemical cycles during infection.<sup>40,107</sup> One of the major differences between phages in soil and aquatic environments is that soils usually contain a higher proportion of temperate phages.<sup>27,108</sup> However, the relative contribution of virulent versus temperate phages to AMGs remains unclear. In this study, both the lysogenic fraction and the number of AMGs carried by temperate phages significantly increased under drought (Figures S9 and 4b). Yet, AMGs were found in similar fractions of virulent and temperate phages (13.37% and 13.82%, respectively), suggesting both phage types were equally important as AMG carriers. Previous studies have reported two viral strategies of modulating microbial metabolisms, i.e., “plunder and pillage” and “batten down the hatches”.<sup>109</sup> The former was typically associated with virulent viruses, which could use AMGs to hijack host metabolism and rewire intracellular resources for progeny production, especially when the hosts are in high density.<sup>110,111</sup> The latter strategy was typically associated with temperate viruses, which could enhance host fitness or resistance under unfavorable environments through the expression of AMGs.<sup>21–25</sup> Hence, our results further support the importance of considering AMGs carried by both virulent and temperate phages.

**4.4. Soil Phage-Encoded AMGs Enriched in Biosynthesis-Related Functions.** Recent advances in soil metaviomic sequencing have led to the discovery of abundant phage AMGs associated with diverse metabolic functions.<sup>41</sup> However, metatranscriptomic analyses may provide further evidence for the activities of AMGs carried by phages in the future. Under both drought and control treatments, the enriched phage AMGs were mostly associated with biosyn-

thesis functions (Figures 4 and 5). Under drought, multiple AMGs involved in nucleotide biosynthesis were enriched, including *purD* (phosphoribosylamine-glycine ligase), *purAB* (adenylosuccinate synthase and lyase), and *dut* (dUTP diphosphatase), etc. Specifically, *purAB* is responsible for the biosynthesis of AMP;<sup>112,113</sup> *purD* is involved in *de novo* synthesis of purine;<sup>114</sup> *dut* is involved in the hydrolysis of dUTP to dUMP.<sup>115</sup> *DNMT1* (DNA (cytosine-5)-methyltransferase 1), catalyzing the degradation of methionine<sup>116</sup> and essential for the maintenance of genomic DNA methylation<sup>117</sup> was also enriched under drought.<sup>56</sup> In addition, AMGs participating in tetrahydrobiopterin biosynthesis were enriched as well, which are involved in multimetabolic processes including electron transfer, amino acid metabolism, hormone synthesis, et cetera.<sup>118</sup> These findings suggest that the phage AMGs might promote nucleic acid metabolism in prokaryotic hosts under drought. Similar findings were proposed to relate to the maintenance of host nucleic acid replication levels and cell proliferation.<sup>119</sup>

Under control, multiple genes involved in carbohydrate metabolism were enriched, including *GME* (GDP-D-mannose 3', 5'-epimerase),<sup>120</sup> *UGDH* (UDP-glucose 6-dehydrogenase),<sup>121</sup> as well as *rfbB* (dTDP-glucose 4,6-dehydratase) and *rfbD* (dTDP-4-dehydrorhamnose reductase) responsible for the biosynthesis of dTDP-L-rhamnose. dTDP-L-rhamnose is a nucleotide sugar that serves as the precursor for the synthesis of rhamnose-containing polysaccharides, which are essential components of bacterial cell walls.<sup>122</sup> Notably, several genes participating in the nonoxidative phase of the pentose phosphate pathway (PPP) were also enriched in phage AMGs (Figure 5), such as *TALDO1* (transaldolase), *rpiB* (ribose 5-phosphate isomerase B), etc. PPP is an important part of central carbon metabolism, generating NADPH, as well as pentoses including ribose-5-phosphate, the precursor for nucleotide biosynthesis.<sup>123</sup> The NADPH produced by PPP is essential for anabolism and the synthesis of large molecules, as well as for the maintenance of cellular redox balance.<sup>124</sup> Studies have found that some marine cyanophages can promote PPP in cyanobacteria after infection, accelerating the production of nucleotides and NADPH, hence facilitating the synthesis of phage nucleotides and particles.<sup>125</sup> Notably, the nonoxidative phase of PPP partly overlaps with the Calvin-Benson-Bassham cycle (CBB).<sup>126</sup> Therefore, AMGs encoding the associated genes may also affect carbon fixation processes in autotrophic hosts (Figure 5).

In summary, our results unveiled the substantial effect of drought on soil phage communities and their interactions with soil prokaryotes. Drought significantly reduced the abundance while increasing the fraction of temperate phages due to its negative effect on soil microbial growth. Drought also enhanced the negative interactions between soil prokaryotes and phages according to profiling of co-occurrence networks and antiphage defense systems. These negative associations primarily target typical *k*-strategists *Acidobacteria* and *Chloroflexi*, whose growth was relatively favored under drought. Phage AMGs were carried in similar fractions of virulent and temperate phages and were enriched in biosynthesis-related functions. These results improved our understanding of prokaryote–phage interactions and phage regulatory mechanisms in the context of global climate change. Moreover, findings of this study demonstrate a profound influence of soil moisture level on soil phages, which must be meticulously managed during soil microbiome manipulation practices.

## ASSOCIATED CONTENT

### Supporting Information

The Supporting Information is available free of charge at <https://pubs.acs.org/doi/10.1021/acs.est.4c08448>.

Results for Epifluorescence microscopy counting and soil moisture of samples; the schematic diagram of sample collection and data processing; the compositions and proportion of vOTUs in samples; the effect of drought on prokaryotic and phage communities; the correlation between mOTU and vOTU numbers and the vOTUs with significantly differentiated abundance under drought; the associations of antiphage defense systems with prokaryotic hosts; the overall properties of nodes in the drought and control networks; the proportion and alpha index of temperate and virulent phages in the samples ([PDF](#))

## AUTHOR INFORMATION

### Corresponding Author

**Jie Deng** — *Zhejiang Tiantong Forest Ecosystem National Observation and Research Station, Center for Global Change and Ecological Forecasting, School of Ecological and Environmental Sciences, East China Normal University, Shanghai 200241, China; Shanghai Key Lab for Urban Ecological Processes and Eco-Restorations, Shanghai 200241, China; Institute of Eco-Chongming, Shanghai 200241, China; Phone: + 86 (21)-54341131; Email: [jdeng@des.ecnu.edu.cn](mailto:jdeng@des.ecnu.edu.cn)*

### Authors

**Cong Liu** — *Zhejiang Tiantong Forest Ecosystem National Observation and Research Station, Center for Global Change and Ecological Forecasting, School of Ecological and Environmental Sciences, East China Normal University, Shanghai 200241, China; Shanghai Key Lab for Urban Ecological Processes and Eco-Restorations, Shanghai 200241, China; [orcid.org/0000-0003-2242-6830](https://orcid.org/0000-0003-2242-6830)*

**Zhijie Chen** — *Zhejiang Tiantong Forest Ecosystem National Observation and Research Station, Center for Global Change and Ecological Forecasting, School of Ecological and Environmental Sciences, East China Normal University, Shanghai 200241, China; [orcid.org/0000-0002-5416-3345](https://orcid.org/0000-0002-5416-3345)*

**Xinlei Wang** — *Zhejiang Tiantong Forest Ecosystem National Observation and Research Station, Center for Global Change and Ecological Forecasting, School of Ecological and Environmental Sciences, East China Normal University, Shanghai 200241, China; [orcid.org/0000-0002-6542-3333](https://orcid.org/0000-0002-6542-3333)*

**Yijun Deng** — *Zhejiang Tiantong Forest Ecosystem National Observation and Research Station, Center for Global Change and Ecological Forecasting, School of Ecological and Environmental Sciences, East China Normal University, Shanghai 200241, China*

**Linfang Tao** — *Zhejiang Tiantong Forest Ecosystem National Observation and Research Station, Center for Global Change and Ecological Forecasting, School of Ecological and Environmental Sciences, East China Normal University, Shanghai 200241, China*

**Xuhui Zhou** — *Northeast Asia Ecosystem Carbon Sink Research Center (NACC), Key Laboratory of Sustainable Forest Ecosystem Management-Ministry of Education, School*

*of Forestry, Northeast Forestry University, Harbin 150040, China; Zhejiang Tiantong Forest Ecosystem National Observation and Research Station, Center for Global Change and Ecological Forecasting, School of Ecological and Environmental Sciences, East China Normal University, Shanghai 200241, China*

Complete contact information is available at: <https://pubs.acs.org/10.1021/acs.est.4c08448>

### Notes

The authors declare no competing financial interest.

## ACKNOWLEDGMENTS

This work was supported by the Natural Science Foundation of China (grant numbers 42177098, 31800424, and 31930072), the Shanghai Pilot Program for Basic Research (TQ20220102), and the Fundamental Research Funds for the Central Universities.

## REFERENCES

- (1) Paez-Espino, D.; Eloe-Fadrosh, E. A.; Pavlopoulos, G. A.; Thomas, A. D.; Huntemann, M.; Mikhailova, N.; Rubin, E.; Ivanova, N. N.; Kyrpides, N. C. Uncovering Earth's virome. *Nature* **2016**, *536*, 425–430.
- (2) Williamson, K. E.; Fuhrmann, J. J.; Wommack, K. E.; Radosevich, M. Viruses in soil ecosystems: An unknown quantity within an unexplored territory. *Annu. Rev. Virol.* **2017**, *4*, 201–219.
- (3) Graham, E. B.; Camargo, A. P.; Wu, R.; Neches, R. Y.; Nolan, M.; Paez-Espino, D.; Kyrpides, N. C.; Jansson, J. K.; McDermott, J. E.; Hofmockel, K. S. A global atlas of soil viruses reveals unexplored biodiversity and potential biogeochemical impacts. *Nat. Microbiol.* **2024**, *9*, 1873–1883.
- (4) Kuzyakov, Y.; Mason-Jones, K. Viruses in soil: Nano-scale undead drivers of microbial life, biogeochemical turnover and ecosystem functions. *Soil Biol. Biochem.* **2018**, *127*, 305–317.
- (5) Pratama, A. A.; van Elsas, J. D. The 'neglected' soil virome – potential role and impact. *Trends Microbiol.* **2018**, *26*, 649–662.
- (6) Proctor, L. M.; Fuhrman, J. A. Viral mortality of marine bacteria and cyanobacteria. *Nature* **1990**, *343*, 60–62.
- (7) Suttle, C. A. Marine viruses – major players in the global ecosystem. *Nat. Rev. Microbiol.* **2007**, *5*, 801–812.
- (8) Han, L.; Yu, D.; Bi, L.; Du, S.; Silveira, C.; Cobian Güemes, A. G.; Zhang, L.; He, J.; Rohwer, F. Distribution of soil viruses across China and their potential role in phosphorous metabolism. *Environ. Microbiome* **2022**, *17*, 6.
- (9) Jin, M.; Guo, X.; Zhang, R.; Qu, W.; Gao, B.; Zeng, R. Diversities and potential biogeochemical impacts of mangrove soil viruses. *Microbiome* **2019**, *7*, 58.
- (10) Kieft, K.; Zhou, Z.; Anderson, R. E.; Buchan, A.; Campbell, B. J.; Hallam, S. J.; Hess, M.; Sullivan, M. B.; Walsh, D. A.; Roux, S.; et al. Ecology of inorganic sulfur auxiliary metabolism in widespread bacteriophages. *Nat. Commun.* **2021**, *12*, 3503.
- (11) Liang, J.; Feng, S.; Lu, J.; Wang, X.; Li, F.; Guo, Y.; Liu, S.; Zhuang, Y.; Zhong, S.; Zheng, J.; et al. Hidden diversity and potential ecological function of phosphorus acquisition genes in widespread terrestrial bacteriophages. *Nat. Commun.* **2024**, *15*, 2827.
- (12) Jansson, J. K.; Wu, R. Soil viral diversity, ecology and climate change. *Nat. Rev. Microbiol.* **2023**, *21*, 296–311.
- (13) Zhao, T.; Dai, A. CMIP6 model-projected hydroclimatic and drought changes and their causes in the 21st century. *J. Clim.* **2021**, *35*, 897–921.
- (14) de Vries, F. T.; Griffiths, R. I.; Bailey, M.; Craig, H.; Girlanda, M.; Gweon, H. S.; Hallin, S.; Kaisermann, A.; Keith, A. M.; Kretzschmar, M.; et al. Soil bacterial networks are less stable under drought than fungal networks. *Nat. Commun.* **2018**, *9*, 3033.

(15) Ochoa-Hueso, R.; Collins, S. L.; Delgado-Baquerizo, M.; Hamonts, K.; Pockman, W. T.; Sinsabaugh, R. L.; Smith, M. D.; Knapp, A. K.; Power, S. A. Drought consistently alters the composition of soil fungal and bacterial communities in grasslands from two continents. *Global Change Biol.* **2018**, *24*, 2818–2827.

(16) Trubl, G.; Jang, H. B.; Roux, S.; Emerson, J. B.; Solonenko, N.; Vik, D. R.; Soden, L.; Ellenbogen, J.; Runyon, A. T.; Bolduc, B.; et al. Soil viruses are underexplored players in ecosystem carbon processing. *mSystems* **2018**, *3*, 10–128.

(17) Xu, Q.; Zhang, H.; Vandenkoornhuyse, P.; Guo, S.; Kuzyakov, Y.; Shen, Q.; Ling, N. Carbon starvation raises capacities in bacterial antibiotic resistance and viral auxiliary carbon metabolism in soils. *Proc. Natl. Acad. Sci. U. S. A.* **2024**, *121*, No. e2318160121.

(18) Liu, C.; Ni, B.; Wang, X.; Deng, Y.; Tao, L.; Zhou, X.; Deng, J. Effect of forest soil viruses on bacterial community succession and the implication for soil carbon sequestration. *Sci. Total Environ.* **2023**, *892*, 164800.

(19) Ma, B.; Wang, Y.; Zhao, K.; Stirling, E.; Lv, X.; Yu, Y.; Hu, L.; Tang, C.; Wu, C.; Dong, B.; Xue, R.; Dahlgren, R. A.; Tan, X.; Dai, H.; Zhu, Y.; Chu, H.; Xu, J. Biogeographic patterns and drivers of soil viromes. *Nat. Ecol. Evol.* **2024**, *8*, 717–728.

(20) Williamson, K. E.; Radosevich, M.; Wommack, K. E. Abundance and diversity of viruses in six Delaware soils. *Appl. Environ. Microbiol.* **2005**, *71*, 3119–3125.

(21) Howard-Varona, C.; Hargreaves, K. R.; Abedon, S. T.; Sullivan, M. B. Lysogeny in nature: mechanisms, impact and ecology of temperate phages. *ISME J.* **2017**, *11*, 1511–1520.

(22) Obeng, N.; Pratama, A. A.; Elsas, J. D. V. The significance of mutualistic phages for bacterial ecology and evolution. *Trends Microbiol.* **2016**, *24*, 440–449.

(23) Paul, J. H.; Sullivan, M. B. Marine phage genomics: what have we learned? *Curr. Opin. Biotech.* **2005**, *16*, 299–307.

(24) Tuttle, M. J.; Buchan, A. Lysogeny in the oceans: Lessons from cultivated model systems and a reanalysis of its prevalence. *Environ. Microbiol.* **2020**, *22*, 4919–4933.

(25) Wang, X.; Kim, Y.; Ma, Q.; Hong, S. H.; Pokusaeva, K.; Sturino, J. M.; Wood, T. K. Cryptic prophages help bacteria cope with adverse environments. *Nat. Commun.* **2010**, *1*, 147.

(26) Zablocki, O.; van Zyl, L.; Adriaenssens, E. M.; Rubagotti, E.; Tuffin, M.; Cary, S. C.; Cowan, D.; Wommack, K. E.; Wommack, K. E. High-level diversity of tailed phages, eukaryote-associated viruses, and virophage-like elements in the metaviromes of Antarctic soils. *Appl. Environ. Microbiol.* **2014**, *80*, 6888–6897.

(27) Wu, R.; Davison, M. R.; Nelson, W. C.; Graham, E. B.; Fansler, S. J.; Farris, Y.; Bell, S. L.; Godinez, I.; McDermott, J. E.; Hofmockel, K. S.; et al. DNA Viral Diversity, Abundance, and Functional Potential Vary across Grassland Soils with a Range of Historical Moisture Regimes. *mBio* **2021**, *12* (6), No. e02595–21.

(28) Chow, C. E.; Kim, D. Y.; Sachdeva, R.; Caron, D. A.; Fuhrman, J. A. Top-down controls on bacterial community structure: microbial network analysis of bacteria, T4-like viruses and protists. *ISME J.* **2014**, *8*, 816–829.

(29) Miki, T.; Jacquet, S. Complex interactions in the microbial world: underexplored key links between viruses, bacteria and protozoan grazers in aquatic environments. *Aquat. Microb. Ecol.* **2008**, *51*, 195–208.

(30) Dutill, B. E.; Cassman, N.; McNair, K.; Sanchez, S. E.; Silva, G. G. Z.; Boling, L.; Barr, J. J.; Speth, D. R.; Seguritan, V.; Aziz, R. K.; et al. A highly abundant bacteriophage discovered in the unknown sequences of human faecal metagenomes. *Nat. Commun.* **2014**, *5*, 4498.

(31) Roux, S.; Brum, J. R.; Dutill, B. E.; Sunagawa, S.; Duhaime, M. B.; Loy, A.; Poulos, B. T.; Solonenko, N.; Lara, E.; Poulain, J.; et al. Ecogenomics and potential biogeochemical impacts of globally abundant ocean viruses. *Nature* **2016**, *537*, 689–693.

(32) Bezuidt, O. K. I.; Lebre, P. H.; Pierneef, R.; Leon-Sobrino, C.; Adriaenssens, E. M.; Cowan, D. A.; Van de Peer, Y.; Makhalaanyane, T. P.; Flynn, T. M. Phages actively challenge niche communities in Antarctic soils. *mSystems* **2020**, *5* (3), No. e00234–20.

(33) Gomez, P.; Buckling, A. Bacteria-phage antagonistic coevolution in soil. *Science* **2011**, *332*, 106–109.

(34) Stern, A.; Sorek, R. The phage-host arms race: Shaping the evolution of microbes. *BioEssays* **2011**, *33*, 43–51.

(35) Albery, G. F.; Becker, D. J.; Brierley, L.; Brook, C. E.; Christofferson, R. C.; Cohen, L. E.; Dallas, T. A.; Eskew, E. A.; Fagre, A.; Farrell, M. J.; et al. The science of the host–virus network. *Nat. Microbiol.* **2021**, *6*, 1483–1492.

(36) Poisot, T.; Ouellet, M. A.; Mollentze, N.; Farrell, M. J.; Becker, D. J.; Brierley, L.; Albery, G. F.; Gibb, R. J.; Seifert, S. N.; Carlson, C. J. Network embedding unveils the hidden interactions in the mammalian virome. *Patterns* **2023**, *4*, 100738.

(37) Weiss, S.; Van Treuren, W.; Lozupone, C.; Faust, K.; Friedman, J.; Deng, Y.; Xia, L. C.; Xu, Z. Z.; Ursell, L.; Alm, E. J.; et al. Correlation detection strategies in microbial data sets vary widely in sensitivity and precision. *ISME J.* **2016**, *10*, 1669–1681.

(38) Soffer, N.; Zaneveld, J.; Vega Thurber, R. Phage–bacteria network analysis and its implication for the understanding of coral disease. *Environ. Microbiol.* **2015**, *17*, 1203–1218.

(39) Wu, R.; Davison, M. R.; Gao, Y.; Nicora, C. D.; McDermott, J. E.; Burnum-Johnson, K. E.; Hofmockel, K. S.; Jansson, J. K. Moisture modulates soil reservoirs of active DNA and RNA viruses. *Commun. Biol.* **2021**, *4*, 992.

(40) Sun, M.; Yuan, S.; Xia, R.; Ye, M.; Balcazar, J. L. Underexplored viral auxiliary metabolic genes in soil: Diversity and eco-evolutionary significance. *Environ. Microbiol.* **2023**, *25*, 800–810.

(41) Van Goethem, M. W.; Swenson, T. L.; Trubl, G.; Roux, S.; Northen, T. R.; Martiny, J. B. H. Characteristics of wetting-induced bacteriophage blooms in biological soil crust. *mBio* **2019**, *10*, No. e02287–19.

(42) Emerson, J. B.; Roux, S.; Brum, J. R.; Bolduc, B.; Woodcroft, B. J.; Jang, H. B.; Singleton, C. M.; Soden, L. M.; Naas, A. E.; Boyd, J. A.; et al. Host-linked soil viral ecology along a permafrost thaw gradient. *Nat. Microbiol.* **2018**, *3*, 870–880.

(43) Huang, X.; Zhou, Z.; Liu, H.; Li, Y.; Ge, T.; Tang, X.; He, Y.; Ma, B.; Xu, J.; Anantharaman, K.; Li, Y. Soil nutrient conditions alter viral lifestyle strategy and potential function in phosphorous and nitrogen metabolisms. *Soil Biol. Biochem.* **2024**, *189*, 109279.

(44) Zheng, X.; Jahn, M. T.; Sun, M.; Friman, V. P.; Balcazar, J. L.; Wang, J.; Shi, Y.; Gong, X.; Hu, F.; Zhu, Y. Organochlorine contamination enriches virus-encoded metabolism and pesticide degradation associated auxiliary genes in soil microbiomes. *ISME J.* **2022**, *16*, 1397–1408.

(45) Huang, D.; Yu, P.; Ye, M.; Schwarz, C.; Jiang, X.; Alvarez, P. J. J. Enhanced mutualistic symbiosis between soil phages and bacteria with elevated chromium-induced environmental stress. *Microbiome* **2021**, *9*, 150.

(46) Santos-Medellin, C.; Zinke, L. A.; Ter Horst, A. M.; Gelardi, D. L.; Parikh, S. J.; Emerson, J. B. Viromes outperform total metagenomes in revealing the spatiotemporal patterns of agricultural soil viral communities. *ISME J.* **2021**, *15*, 1956–1970.

(47) Kosmopoulos, J. C.; Klier, K. M.; Langwig, M. V.; Tran, P. Q.; Anantharaman, K. Viromes vs. mixed community metagenomes: choice of method dictates interpretation of viral community ecology. *Microbiome* **2024**, *12*, 195.

(48) Zhou, G.; Zhou, X.; Zhang, T.; Du, Z.; He, Y.; Wang, X.; Shao, J.; Cao, Y.; Xue, S.; Wang, H.; Xu, C. Biochar increased soil respiration in temperate forests but had no effects in subtropical forests. *For. Ecol. Manage.* **2017**, *405*, 339–349.

(49) Su, X.; Su, X.; Yang, S.; Zhou, G.; Ni, M.; Wang, C.; Qin, H.; Zhou, X.; Deng, J. Droughtchanged soil organic carbon composition and bacterial carbon metabolizing patterns in a subtropical evergreen forest. *Sci. Total Environ.* **2020**, *736*, 139568.

(50) Su, X.; Su, X.; Zhou, G.; Du, Z.; Yang, S.; Ni, M.; Qin, H.; Huang, Z.; Zhou, X.; Deng, J. Drought accelerated recalcitrant carbon loss by changing soil aggregation and microbial communities in a subtropical forest. *Soil Biol. Biochem.* **2020**, *148*, 107898.

(51) Bach, E. M.; Hofmockel, K. S. Soil aggregate isolation method affects measures of intra- aggregate extracellular enzyme activity. *Soil Biol. Biochem.* **2014**, *69*, 54–62.

(52) Williamson, K. E.; Radosevich, M.; Smith, D. W.; Wommack, K. E. Incidence of lysogeny within temperate and extreme soil environments. *Environ. Microbiol.* **2007**, *9*, 2563–2574.

(53) Saiya-Cork, K. R.; Sinsabaugh, R. L.; Zak, D. R. The effects of long term nitrogen deposition on extracellular enzyme activity in an *Acer saccharum* forest soil. *Soil Biol. Biochem.* **2002**, *34*, 1309–1315.

(54) Bolger, A. M.; Lohse, M.; Usadel, B. Trimmomatic: a flexible trimmer for Illumina sequence data. *Bioinformatics* **2014**, *30*, 2114–2120.

(55) Li, D.; Liu, C. M.; Luo, R.; Sadakane, K.; Lam, T. W. MEGAHIT: an ultra- fast single- node solution for large and complex metagenomics assembly via succinct de Bruijn graph. *Bioinformatics* **2015**, *31*, 1674–1676.

(56) Hyatt, D.; Chen, G. L.; LoCascio, P. F.; Land, M. L.; Larimer, F. W.; Hauser, L. J. Prodigal: prokaryotic gene recognition and translation initiation site identification. *BMC Bioinform.* **2010**, *11*, 119.

(57) Fu, L.; Niu, B.; Zhu, Z.; Wu, S.; Li, W. CD-HIT: accelerated for clustering the next- generation sequencing data. *Bioinformatics* **2012**, *28*, 3150–3152.

(58) Buchfink, B.; Xie, C.; Huson, D. H. Fast and sensitive protein alignment using DIAMOND. prokaryotic gene recognition and translation initiation site identification. *BMC Bioinform* **2010**, *11*, 119.

(59) Kanehisa, M.; Goto, S. K. KEGG: Kyoto Encyclopedia of Genes and Genomes. *Nucleic Acids Res.* **2000**, *28*, 27–30.

(60) Peng, Y.; Leung, H. C. M.; Yiu, S. M.; Chin, F. Y. L. IDBA-UD: a de novo assembler for single- cell and metagenomic sequencing data with highly uneven depth. *Bioinformatics* **2012**, *28*, 1420–1428.

(61) Guo, J.; Bolduc, B.; Zayed, A. A.; Varsani, A.; Dominguez- Huerta, G.; Delmont, T. O.; Pratama, A. A.; Gazitua, M. C.; Vik, D.; Sullivan, M. B.; et al. VirSorter2: a multi-classifier, expert-guided approach to detect diverse DNA and RNA viruses. *Microbiome* **2021**, *9*, 37.

(62) Ren, J.; Song, K.; Deng, C.; Ahlgren, N. A.; Fuhrman, J. A.; Li, Y.; Xie, X.; Poplin, R.; Sun, F. Identifying viruses from metagenomic data using deep learning. *Quant. Biol.* **2020**, *8*, 64–77.

(63) Kieft, K.; Zhou, Z.; Anantharaman, K. VIBRANT: automated recovery, annotation and curation of microbial viruses, and evaluation of viral community function from genomic sequences. *Microbiome* **2020**, *8*, 90.

(64) Nayfach, S.; Camargo, A. P.; Schulz, F.; Eloë-Fadrosh, E.; Roux, S.; Kyrpides, N. C. CheckV assesses the quality and completeness of metagenome-assembled viral genomes. *Nat. Biotechnol.* **2021**, *39*, 578–585.

(65) Kanehisa, M.; Sato, Y.; Morishima, K. BlastKOALA and GhostKOALA: KEGG tools for functional characterization of genome and metagenome sequences. *J. Mol. Biol.* **2016**, *428*, 726.

(66) Shang, J.; Jiang, J.; Sun, Y. Bacteriophage classification for assembled contigs using graph 731. convolutional network. *Bioinformatics* **2021**, *37*, i25–i33.

(67) Shaffer, M.; Borton, M. A.; McGivern, B. B.; Zayed, A. A.; La Rosa, S. L.; Solden, L. M.; Liu, P.; Narro, A. B.; Rodriguez-Ramos, J.; Bolduc, B.; Gazitua, M. C.; Daly, R. A. DRAM for distilling microbial metabolism to automate the curation of microbiome function. *Nucleic Acids Res.* **2020**, *48*, 8883–8900.

(68) Solovyev, V. V.; Salamov, A. A. Metagenomics and its applications in agriculture, biomedicine and environmental studies. chapterAutomatic annotation of microbial genomes and metagenomic sequencesNova Science Publishers201161–78

(69) Kelley, L. A.; Mezulis, S.; Yates, C. M.; Wass, M. N.; Sternberg, M. J. E. The Phyre2 web portal for protein modeling, prediction and analysis. *Nat. Protoc.* **2015**, *10*, 845–858.

(70) Jahn, M. T.; Lachnit, T.; Markert, S. M.; Stigloher, C.; Pita, L.; Ribes, M.; Dutilh, B. E.; Hentschel, U. Lifestyle of sponge symbiont phages by host prediction and correlative microscopy. *ISME J.* **2021**, *15*, 2001–2011.

(71) Bland, C.; Ramsey, T. L.; Sabree, F.; Lowe, M.; Brown, K.; Kyrpides, N. C.; Hugenholz, P. CRISPR recognition tool (CRT): a tool for automatic detection of clustered regularly interspaced palindromic repeats. *BMC Bioinform.* **2007**, *8*, 209.

(72) Lowe, T. M.; Chan, P. P. tRNAscan-SE On-line: integrating search and context for analysis of transfer RNA genes. *Nucleic Acids Res.* **2016**, *44*, W54–W57.

(73) Edwards, R. A.; McNair, K.; Faust, K.; Raes, J.; Dutilh, B. E. Computational approaches to predict bacteriophage-host relationships. *FEMS Microbiol. Rev.* **2016**, *40*, 258–272.

(74) Cook, R.; Hooton, S.; Trivedi, U.; King, L.; Dodd, C. E. R.; Hobman, J. L.; Stekel, D. J.; Jones, M. A.; Millard, A. D. Hybrid assembly of an agricultural slurry virome reveals a diverse and stable community with the potential to alter the metabolism and virulence of veterinary pathogens. *Microbiome* **2021**, *9*, 65.

(75) Shang, J.; Tang, X.; Sun, Y. PhaTYP: Predicting the lifestyle for bacteriophages using BERT. *Brief. Bioinform.* **2023**, *24*, bbac487.

(76) Tesson, F.; Herve, A.; Mordret, E.; Touchon, M.; d'Humieres, C.; Cury, J.; Bernheim, A. Systematic and quantitative view of the antiviral arsenal of prokaryotes. *Nat. Commun.* **2022**, *13*, 2561.

(77) Wen, T.; Xie, P.; Yang, S.; Niu, G.; Liu, X.; Ding, Z.; Xue, C.; Liu, Y.; Shen, Q.; Yuan, J. ggClusterNet: An R package for microbiome network analysis and modularity-based multiple network layouts. *iMeta* **2022**, *1*, No. e32.

(78) Oksanen, J.; Blanchet, F. G.; Kindt, R.; Legendre, P.; Minchin, P.; O'Hara, B.; Simpson, G.; Solymos, P.; Stevens, H.; Wagner, H. Vegan: Community ecology package: R package version 2561. Scientific Research Publishing Inc., 2015.

(79) Wickham, H. *ggplot2: Elegant graphics for data analysis*. ISBN 978–3–319–24277–4 Springer-Verlag New York. 2016, <https://ggplot2.tidyverse.org>.

(80) Kassambara, A. *ggpubr: ggplot2 based publication ready plots: R package version 0.6.0*. 2023. <https://rpkg.datanovia.com/ggpubr/>.

(81) Robinson, M. D.; McCarthy, D. J.; Smyth, G. K. edgeR: a Bioconductor package for differential expression analysis of digital gene expression data. *Bioinformatics* **2010**, *26*, 139–140.

(82) Cochran, P. K.; Paul, J. H. Seasonal abundance of lysogenic bacteria in a subtropical estuary. *Appl. Environ. Microbiol.* **1998**, *64*, 2308–2312.

(83) Middelboe, M. Bacterial growth rate and marine virus–host dynamics. *Microb. Ecol.* **2000**, *40*, 114–124.

(84) Pradeep Ram, A. S.; Sime-Ngando, T. Resources drive trade-off between viral lifestyles in the plankton: evidence from freshwater microbial microcosms. *Environ. Microbiol.* **2010**, *12*, 467–479.

(85) Shan, J.; Korbsrisate, S.; Withanun, P.; Adler, N. L.; Clokie, M. R. J.; Galyov, E. E. Galyov, E. E. Temperature dependent bacteriophages of a tropical bacterial pathogen. *Front. Microbiol.* **2014**, *5*, 599.

(86) Touchon, M.; Bernheim, A.; Rocha, E. P. Genetic and life-history traits associated with the distribution of prophages in bacteria. *ISME J.* **2016**, *10*, 2744–2754.

(87) Williamson, S. J.; Houchin, L. A.; McDaniel, L.; Paul, J. H. Seasonal variation in lysogeny as depicted by prophage induction in Tampa Bay, Florida. *Appl. Environ. Microbiol.* **2002**, *68*, 4307–4314.

(88) Cleveland, C. C.; Wieder, W. R.; Reed, S. C.; Townsend, A. R. Experimental drought in atropical rain forest increases soil carbon dioxide losses to the atmosphere. *Ecology* **2010**, *91*, 2313–2323.

(89) Zhou, G.; Zhou, X.; Nie, Y.; Bai, S. H.; Zhou, L.; Shao, J.; Cheng, W.; Wang, J.; Hu, F.; Fu, Y. Drought-induced changes in root biomass largely result from altered root morphological traits: Evidence from a synthesis of global field trials. *Plant Cell Environ.* **2018**, *41*, 2589–2599.

(90) Huang, D.; Xia, R.; Chen, C.; Liao, J.; Chen, L.; Wang, D.; Alvarez, P. J. J.; Yu, P. Adaptive strategies and ecological roles of phages in habitats under physicochemical stress. *Trends Microbiol.* **2024**, *32*, 902–916.

(91) Pan, Y.; Kang, P.; Tan, M.; Hu, J.; Zhang, Y.; Zhang, J.; Song, N.; Li, X. Root exudates and rhizosphere soil bacterial relationships of

Nitraria tangutorum are linked to k-strategists bacterial community under salt stress. *Front. Plant Sci.* **2022**, *13*, 1–15.

(92) Fierer, N.; Bradford, M. A.; Jackson, R. B. Toward an ecological classification of soil bacteria. *Ecology* **2007**, *88*, 1354–1364.

(93) Bongers, T. The maturity index, the evolution of nematode life history traits, adaptive radiation and cp-scaling. *Plant Soil* **1999**, *212*, 13–22.

(94) Wang, J.; Wang, C.; Wu, X.; Zhang, J.; Zhao, G.; Hou, Y.; Sun, H. Effects of moderate droughtextension on bacterial network structure in the rhizosphere soil of Leymus chinensis in semi-arid grasslands. *Front. Microbiol.* **2023**, *14*, 1217557.

(95) Rawat, S. R.; Männistö, M. K.; Bromberg, Y.; Häggblom, M. M. Comparative genomic andphysiological analysis provides insights into the role of Acidobacteria in organic carbon utilization in Arctic tundra soils. *FEMS Microbiol. Ecol.* **2012**, *82*, 341–355.

(96) Ward, N. L.; Challacombe, J. F.; Janssen, P. H.; Henrissat, B.; Coutinho, P. M.; Wu, M.; Xie, G.; Haft, D. H.; Sait, M.; Badger, J.; et al. Three genomes from the phylum Acidobacteria provide insight into the lifestyles of these microorganisms in soils. *Appl. Environ. Microbiol.* **2009**, *75*, 2046–2056.

(97) Hu, P.; Zhang, W.; Kuzyakov, Y.; Xiao, L.; Xiao, D.; Xu, L.; Chen, H.; Zhao, J.; Wang, K. Linking bacterial life strategies with soil organic matter accrual by karst vegetation restoration. *Soil Biol. Biochem.* **2023**, *177*, 108925.

(98) Oliveira, P. H.; Touchon, M.; Rocha, E. P. The interplay of restriction-modification systems with mobile genetic elements and their prokaryotic hosts. *Nucleic Acids Res.* **2014**, *42*, 10618–10631.

(99) Bertani, G.; Weigle, J. J. Host Controlled variation in bacterial viruses. *J. Bacteriol.* **1953**, *65*, 113–121.

(100) Millman, A.; Melamed, S.; Leavitt, A.; Doron, S.; Bernheim, A.; Hör, J.; Garb, J.; Bechon, N.; Brandis, A.; Lopatina, A.; et al. An expanded arsenal of immune systems that protect bacteria from phages. *Cell Host Microbe.* **2022**, *30*, 1556–1569.E5.

(101) Makarova, K. S.; Wolf, Y. I.; van der Oost, J.; Koonin, E. V. Prokaryotic homologs ofArgonaute proteins are predicted to function as key components of a novel system of defense against mobile genetic elements. *Biol. Direct.* **2009**, *4* (1), 29.

(102) Bobadilla Ugarde, P.; Barendse, P.; Swarts, D. C. Argonaute proteins confer immunity in all domains of life. *Curr. Opin. Microbiol.* **2023**, *74*, 102313.

(103) Millman, A.; Melamed, S.; Amitai, G.; Sorek, R. Diversity and classification of cyclic- oligonucleotide-based anti-phage signalling systems. *Nat. Microbiol.* **2020**, *5*, 1608–1615.

(104) Kogay, R.; Wolf, Y. I.; Koonin, E. V. Defence systems and horizontal gene transfer in bacteria. *Environ. Microbiol.* **2024**, *26*, No. e16630.

(105) Wang, X.; Zhou, L.; Fu, Y.; Jiang, Z.; Jia, S.; Song, B.; Liu, D.; Zhou, X. Drought-inducedchanges in rare microbial community promoted contribution of microbial necromass C to SOC in a subtropical forest. *Soil Biol. Biochem.* **2024**, *189*, 109252.

(106) Wang, X.; Zhou, L.; Zhou, G.; Zhou, H.; Lu, C.; Gu, Z.; Liu, R.; He, Y.; Du, Z.; Liang, X.; He, H.; Zhou, X. Tradeoffs of fungal and bacterial residues mediate soil carbon dynamics under persistent drought in subtropical evergreen forests. *Appl. Soil Ecol.* **2022**, *178*, 104588.

(107) Jacobson, T. B.; Callaghan, M. M.; Amador-Noguez, D. Hostile takeover: How viruses reprogram prokaryotic metabolism. *Annu. Rev. Microbiol.* **2021**, *75*, 515–539.

(108) Ghosh, D.; Roy, K.; Williamson, K. E.; White, D. C.; Wommack, K. E.; Sublette, K. L.; Radosevich, M. Prevalence of lysogeny among soil bacteria and presence of 16S rRNA and trzN genes in viral-community DNA. *Appl. Environ. Microbiol.* **2008**, *74*, 495–502.

(109) Warwick-Dugdale, J.; Buchholz, H. H.; Allen, M. J.; Temperton, B. Host-hijacking and planktonic piracy: how phages command the microbial high seas. *Virol. J.* **2019**, *16*, 15.

(110) Howard-Varona, C.; Lindback, M. M.; Bastien, G. E.; Solonenko, N.; Zayed, A. A.; Jang, H.; Andreopoulos, B.; Brewer, H. M.; Glavina Del Rio, T.; Adkins, J. N.; Paul, S.; Sullivan, M. B.; Duhamel, M. B. Phage-specific metabolic reprogramming of virocells. *ISME J.* **2020**, *14*, 881–895.

(111) Lindell, D.; Jaffe, J. D.; Johnson, Z. I.; Church, G. M.; Chisholm, S. W. Photosynthesis genes in marine viruses yield proteins during host infection. *Nature* **2005**, *438*, 86–89.

(112) Powell, S. M.; Zalkin, H.; Dixon, J. E. Cloning and characterization of the cDNA encoding human adenylosuccinate synthetase. *FEBS Lett.* **1992**, *303*, 4–10.

(113) Tsai, M.; Koo, J.; Yip, P.; Colman, R. F.; Segall, M. L.; Howell, P. L. Substrate and productcomplexes of Escherichia coli adenylosuccinate lyase provide new insights into the enzymatic mechanism. *J. Mol. Biol.* **2007**, *370*, 541–554.

(114) Aiba, A.; Mizobuchi, K. Nucleotide sequence analysis of genes purH and purD involved in the de novo purine nucleotide biosynthesis of Escherichia coli. *J. Biol. Chem.* **1989**, *264*, 21239–21246.

(115) Ladner, R. D.; McNulty, D. E.; Carr, S. A.; Roberts, G. D.; Caradonna, S. J. Characterizationof distinct nuclear and mitochondrial forms of human deoxyuridine triphosphate nucleotidohydrolase. *J. Biol. Chem.* **1996**, *271*, 7745–7751.

(116) Militello, K. T.; Simon, R. D.; Qureshi, M.; Maines, R.; Van Horne, M. L.; Hennick, S. M.; Jayakar, S. K.; Pounder, S. Conservation of Dcm-mediated cytosine DNA methylation in Escherichia coli. *FEMS Microbiol. Lett.* **2012**, *328*, 78–85.

(117) Hermann, A.; Goyal, R.; Jeltsch, A. The Dnmt1 DNA-(cytosine-C5)- methyltransferase methylates DNA processively with high preference for hemimethylated target sites. *J. Biol. Chem.* **2004**, *279*, 48350–48359.

(118) Thöny, B.; Auerbach, G.; Blau, N. Tetrahydrobiopterin biosynthesis, regeneration and functions. *Biochem. J.* **2000**, *347*, 1–16.

(119) Luo, X.; Wang, P.; Li, J.; Ahmad, M.; Duan, L.; Yin, L.; Deng, Q.; Fang, B.; Li, S.; Li, W. Viral community-wide auxiliary metabolic genes differ by lifestyles, habitats, and hosts. *Microbiome* **2022**, *10*, 190.

(120) Watanabe, K.; Suzuki, K.; Kitamura, S. Characterization of a GDP-d-mannose 3",5"- epimerase from rice. *Phytochemistry* **2006**, *67*, 338–346.

(121) Sennett, N. C.; Kadirvelraj, R.; Wood, Z. A. Conformational flexibility in the allosteric regulation of human UDP- $\alpha$ -d-Glucose 6-Dehydrogenase. *Biochemistry* **2011**, *50*, 9651–9663.

(122) van der Beek, S. L.; Zorzoli, A.; Canak, E.; Chapman, R. N.; Lucas, K.; Meyer, B. H.; Evangelopoulos, D.; de Carvalho, L. P. S.; Boons, G. J.; Dorfmüller, H. C.; van Sorge, N. M. Streptococcal dTDP-L- rhamnose biosynthesis enzymes: functional characterization and lead compound identification. *Mol. Microbiol.* **2019**, *111*, 951–964.

(123) Alfarouk, K. O.; Ahmed, S. B. M.; Elliott, R. L.; Benoit, A.; Alqahtani, S. S.; Ibrahim, M. E.; Bashir, A. H. H.; Alhoufie, S. T. S.; Elhassan, G. O.; Wales, C. C.; et al. The pentose phosphate pathway dynamics in Cancer and its dependency on intracellular pH. *Metabolites* **2020**, *10*, 285.

(124) Stincone, A.; Prigione, A.; Cramer, T.; Wamelink, M. M.; Campbell, K.; Cheung, E.; Olin- Sandoval, V.; Gruning, N. M.; Kruger, A.; Tauqeer Alam, M.; Keller, M. A.; Breitenbach, M.; Brindle, K. M.; Rabinowitz, J. D.; Ralser, M. The return of metabolism: biochemistry and physiology of the pentose phosphate pathway. *Biol. Rev. Camb Philos. Soc.* **2015**, *90*, 927–963.

(125) Thompson, L. R.; Zeng, Q.; Kelly, L.; Huang, K. H.; Singer, A. U.; Stubbe, J.; Chisholm, S. W. Phage auxiliary metabolic genes and the redirection of cyanobacterial host carbon metabolism. *Proc. Natl. Acad. Sci. U. S. A.* **2011**, *108*, No. E757–E764.

(126) Garrett, R. H.; Grisham, C. M. *Biochemistry*; Cengage Learning, 2008.